

## Transfer and tissue-specific accumulation of cytoplasmic components in embryos of *Caenorhabditis elegans* and *Rhabditis dolichura*: in vivo analysis with a low-cost signal enhancement device

OLAF BOSSINGER and EINHARD SCHIERENBERG

Zoologisches Institut der Universität Köln, Weyertal 119, 5000 Köln 41, Federal Republic of Germany

### Summary

The pattern of autofluorescence in the two free-living soil nematodes *Rhabditis dolichura* and *Caenorhabditis elegans* has been compared. In *C. elegans*, during later embryogenesis the prospective gut cells develop a typical bluish autofluorescence as seen under UV illumination, while in *Rh. dolichura* a strong autofluorescence is already present in the unfertilized egg. Using a new, low-cost signal enhancement device, we have been able to follow in vivo the dramatic change in the pattern of autofluorescence during embryogenesis of *Rh. dolichura*. Autofluorescent material accumulates progressively in the gut primordium and disappears completely from all other cells. To investigate whether such an accumulation of cytoplasmic components also takes place in the *C. elegans* embryo, we labeled the cytoplasm of the egg with the fluorescing tracer dyes Lucifer Yellow (LY) or Rhodamine 6G (R6G). While LY appears to bind to yolk and progressively accumulates in the

developing gut primordium, R6G does not show any such binding and remains equally distributed over all cells. Measurements in early and late stages indicate a significant increase in the volume of the gut cells during embryogenesis, while the embryo as a whole does not grow. Moreover, in cleavage-blocked 2-cell stages after development overnight, a reversal of cell size relationship to the benefit of the gut precursor cell takes place. In summary, our observations suggest a previously unknown massive transfer of yolk components in the nematode embryo from non-gut cells into lysosomes of the gut primordium, where they are further metabolized during postembryonic development.

Key words: *C. elegans*, nematode, gut differentiation, autofluorescence, yolk, microinjection, Lucifer Yellow, Rhodamine, video enhancement.

### Introduction

During embryogenesis of the nematode *C. elegans* characteristic signs of tissue-specific differentiation develop. One prominent differentiation marker is a bluish autofluorescence under UV illumination, which appears in the gut lineage, three to four hours after the onset of cleavage when eight gut precursor cells have been formed (8 E-cell stage; Deppe et al., 1978). Development of this differentiation marker is not dependent on cell division (Laufer et al., 1980), but zygotic expression of the appropriate genes is necessary (Edgar and McGhee, 1986, 1988). Mutants affecting the degradation pathway of tryptophan show an altered color and intensity of autofluorescence (Babu, 1974; Siddiqui and Babu, 1980). There are indications that these granules are lysosomes, which take up exogenous macromolecules by fluid-phase pinocytosis (Clokey and Jacobson, 1986).

We are interested in the process leading to the formation of autofluorescent gut granules during embryogenesis, particularly whether they derive from the

original products of the intestine or whether they are imported from other cells. Therefore, we have started to analyze a number of different nematode species closely related to *C. elegans*. (1) We describe the pattern of autofluorescence in the embryo of *Rh. dolichura*, which differs from that observed in *C. elegans*. (2) We show that the dye Lucifer Yellow (Stewart, 1978) can be used as a fluorescence marker to visualize a stage-specific transfer and uptake of certain molecules into the gut of the *C. elegans* embryo, which demonstrates that a process similar if not identical to that in *Rh. dolichura* takes place. (3) We document that transfer and accumulation of cytoplasmic components become particularly obvious in cleavage-blocked embryos, showing that cell division is not necessary for this tissue-specific differentiation.

### Materials and methods

#### *Nematode strains and maintenance*

*C. elegans* (var. Bristol) strain N2 and *Rh. dolichura* were

raised on nutrient agar plates with a uracil-deficient strain of *E. coli* (OP 50) as a food source, essentially as described by Brenner (1974).

#### *In vivo labelling with Rhodamine 6G and Lucifer Yellow VS*

##### *Rhodamine*

Worms were incubated with a concentration of  $10^{-4}\%$  R6G (relative molecular mass  $M_r$  479; absorption max.: 526 nm; Merck, Darmstadt) on nutrient agar plates overnight.

##### *Lucifer Yellow*

Worms were incubated in cell culture medium (see below) complemented with 2.5% LYVS ( $M_r$  457; absorption max.: 436 nm; Sigma) and a low concentration of *E. coli* as a food source for a few hours at room temperature. The dye was taken up orally by the feeding worms together with the bacteria and transferred from the intestine into the oocytes. After incubation, the fluorescently labelled eggs were prepared for microscopy and centrifugation as described below.

#### *Microinjection of Lucifer Yellow into early blastomeres*

Embryos of appropriate stages were attached to polylysine-coated coverslips and covered with cell-culture medium (see below) and 8S fluorocarbon oil to prevent evaporation. Under an inverted microscope (Leitz Diavert) with an Olympus 40× APO UV oil immersion objective, selected blastomeres of early-stage embryos were iontophoretically injected with a 2.5% solution of Lucifer Yellow VS (LYVS) in aqua dest.

#### *Introduction of Lucifer Yellow into the perivitelline space with a laser microbeam*

Embryos were attached to a microscope slide as described above and preincubated with a saturated solution of Trypan Blue (Merck, Darmstadt) for a few minutes. The dye adheres to the eggshell and allows absorption of the orange laser microbeam. Then the dye solution was replaced by cell culture medium (see below) containing 0.25% LYVS. The eggshell and underlying vitelline membrane were penetrated with a single laser pulse (Laufer and von Ehrenstein, 1981; Schierenberg and Wood, 1985) to allow entry of the dye into the perivitelline space. After 5-10 minutes, the dye-containing medium was exchanged for the same medium without LYVS. Dye in the perivitelline space was not lost this way, probably because the vitelline membrane had resealed in the meantime.

#### *Microscopy of living embryos*

Eggs were dissected out of gravid adults with a scalpel in a drop of distilled water on a microscope slide. Uncleaved zygotes were identified under the dissecting microscope and transferred with a drawn-out glass mouth pipette to a second microscope slide carrying a thin layer of 3-5% agar in  $H_2O$  as a cushion. The eggs were covered with a coverslip and the edges sealed with Vaseline (Sulston and Horvitz, 1977; Deppe et al., 1978). Development of embryos was observed with Nomarski optics and epi-illumination at 340-380 nm (autofluorescence; filter combination A), 436 nm (LYVS; filter combination E), and 520-560 nm (R6G; filter combination N2), using a 40× UV oil immersion objective. To allow reproducible short exposure times, a remote-controlled shutter was placed between the mercury bulb and the microscope.

#### *Centrifugation of embryos*

Embryos of appropriate stages were selected under a dissecting microscope (as described above) and transferred to a polylysine-coated microscope slide. Centrifugation in cell culture medium (see below) was performed at 4500 g for 5 minutes at 10°C using a custom-made plastic holder to prevent breakage of the microscope slide during centrifugation. This method has been described in more detail elsewhere (Schlicht and Schierenberg, 1991).

#### *Blocking cleavage in early embryos*

Cell division of 2-cell stages was inhibited by adding 5 µg/ml cytochalasin D to the cell culture medium (described below). To allow penetration of cytochalasin, the impermeable eggshell was punctured with a laser microbeam as described above.

#### *Cell culture medium*

The medium used to support development of ruptured embryos (Cole and Schierenberg, 1986) consisted of 50% BM 86 Wissler (Boehringer, Mannheim), 30% Dulbecco's MEM/Ham's F-12 (Sigma), 15% fetal calf serum (Sigma) and 5% penicillin (5,000 units/ml)-streptomycin (5 mg/ml; Sigma).

#### *Calculation of cell volumes*

##### *Volume of the gut founder cell E and its daughters Ea and Ep*

From prints of three longitudinal electron microscopic section series, the relative volume of E (8-cell stage) and its two daughters (14-, 24-cell stages) was calculated with the help of a data tablet connected to a PDP 11/45 computer (Schierenberg, 1978). The surface of the whole embryo and that of the E cell (or its daughters) were measured in every third to fifth section and multiplied correspondingly by 3-5 to take the omitted sections into account. To compensate for variations in natural size and fixation artefacts, embryos were normalized to give the same total volume.

##### *Volume of the intestine in late embryos and freshly hatched juveniles*

On individual electron micrographs of transverse sections through various regions of a young L1 stage larva and a "pretzel" stage (late morphogenesis stage; see Fig. 7D), we measured the surface occupied by the gut cell cytoplasm (as % of total surface) with the help of a data tablet connected to an Apple IIe computer. To obtain relative volumes, these data were multiplied by the relative length of the intestine (as % of total animal length, excluding tail) measured in young L1 stage larvae under the light microscope.

#### *Video recording, electronic enhancement and photography*

Living embryos were recorded on an AG 6720 Panasonic Super-VHS time-lapse recorder with a Panasonic WV BL 600 CCD camera and a WV CU 204 camera-control unit. After activation of the electronic "Sensitivity Up" mode, the appropriate level of enhancement was selected manually prior to recording. To document appearance and localization of autofluorescence in individual embryos, these were briefly exposed to UV light and simultaneously recorded for 0.25-1 seconds approximately once every hour. Selected images of the recorded specimens were photographed from the running screen or at stop-motion mode with Ilford HP 5 (400 ASA) black and white film at shutter speed 0.25 seconds.

### Number of observations and experiments

Each observation described in this paper has been made on at least 10 different individuals unless mentioned otherwise.

## Results

### *Simultaneous display of many electronically accumulated images allows visualization of low level autofluorescence in the gut primordium*

The camera that we use, together with its accompanying control board, allows storage of up to 32 video images in a picture memory, which can be displayed simultaneously on the video screen. The collective display of multiple images results in the enhancement of the light signal relative to noise, allowing visualization of weakly fluorescing structures, which cannot (or hardly) be seen by direct observation or be picked up by a conventional video camera. Fig. 1 demonstrates this feature by visualizing the just arising gut-specific autofluorescence in a *C. elegans* embryo at increasing levels of enhancement (i.e. number of simultaneously displayed images).

### *Contrast-enhanced videorecording permits short exposure to fluorescence excitation*

To visualize (a) autofluorescence, (b) Lucifer Yellow (LYVS) or (c) Rhodamine 6G (R6G)-induced fluorescence in nematode embryos, they must be irradiated with light of 340-380 nm (a), 436 nm (b) or 520-560 nm (c), respectively. However, the autofluorescence in *Rh. dolichura* bleaches out within a few seconds (not allowing proper documentation even with high-speed film). In addition, repeated irradiation - even if only for a few seconds - usually causes immediate or later

developmental arrest of the embryos. With video recording as described in Materials and methods, exposure times as low as 0.3 seconds are sufficient for proper documentation. Such brief exposure to harmful light can be tolerated by the embryos so the pattern of fluorescence can be traced in individual specimens from early cleavage to hatching.

### *In the *C. elegans* embryo autofluorescence becomes visible in the gut primordium several hours after the onset of cleavage*

We have traced the appearance of bluish autofluorescence in the *C. elegans* embryo. By direct observation, it can be clearly identified in the gut primordium consisting of 16 descendants of the intestinal founder cell "E" (16 E-cell stage; >300 cells in total; Sulston et al., 1983). Even with 32× image enhancement the 1 to 4 E-cell stages (<100 cells) display only a very faint pale background fluorescence (Fig. 2a-c). From the 8 E-cell stage onwards (>200 cells), an increasingly stronger bluish autofluorescence from distinct granules shows up in the gut primordium (Fig. 2d-f).

From these observations, it is not clear whether the fluorescent structures are formed tissue-autonomously by the intestine or if transfer processes into the gut are involved. Therefore, we analyzed the patterns of autofluorescence in other free-living nematodes.

### *In *Rh. dolichura* autofluorescence is already present in the unfertilized egg and accumulates in the gut primordium during embryogenesis*

In contrast to *C. elegans*, a bluish autofluorescence is present equally in the cytoplasm all over the *Rh. dolichura* egg even prior to fertilization. This becomes particularly obvious after electronic enhancement, but

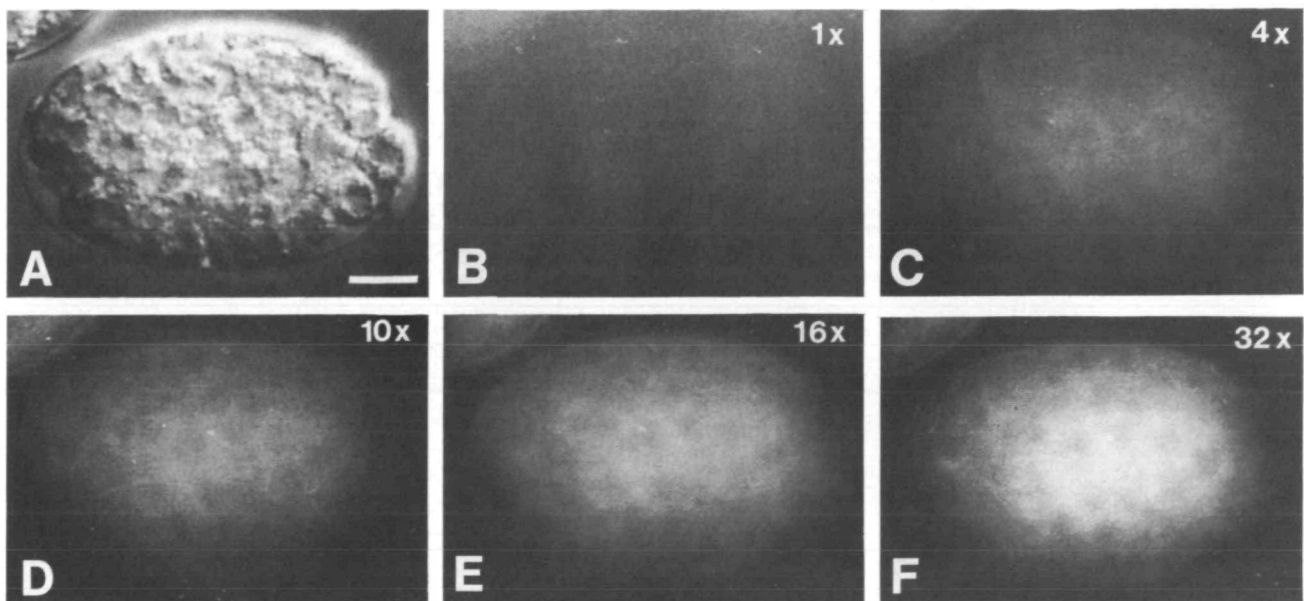


**Fig. 1.** Visualization of low-level fluorescence employing a camera with picture memory. (A) 8 E-cell stage embryo of *C. elegans* (approx. 150 cells in total), Nomarski optics. (B-F) Same embryo, same stage as in A, epifluorescence, different steps of signal enhancement. Autofluorescence of E (gut precursor) cells becomes clearly visible only at maximal possible intensification. Factor of enhancement given in top right corner of each image. Bar: 10  $\mu$ m. Orientation: anterior, left.

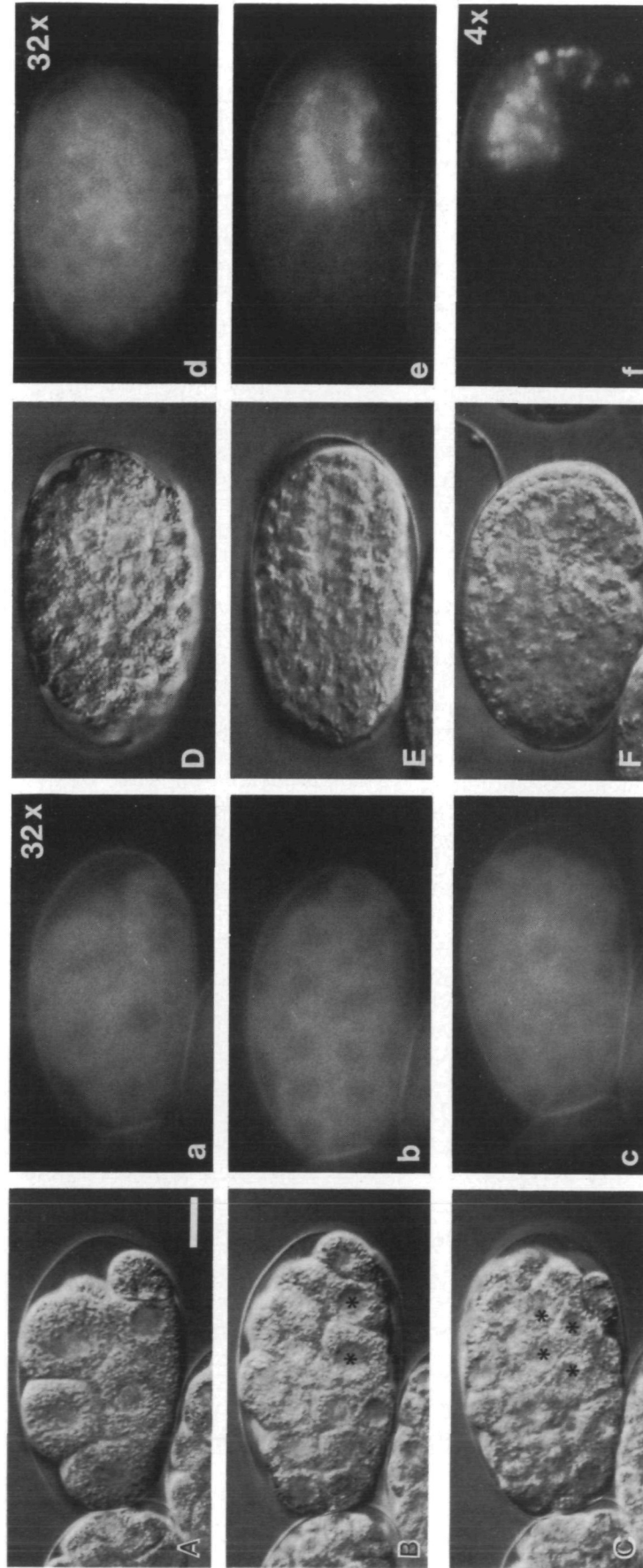


**Fig. 2.** Development of autofluorescence in the *C. elegans* embryo. (A,a) 8-cell stage (1 E-cell). (B,b) 26-cell stage (2 E-cells). (C,c) 4 E-cell stage. (D,d) 8 E-cell stage. (E,e) 16 to 20 E-cell stage. (F,f) Early morphogenesis stage (20 E-cells), asterisks mark the two (B) or four (C) E cells present at the respective corner. Bar: 10  $\mu$ m. Orientation: anterior, left.

**Fig. 2.** In the following stages, the position of E cells can be deduced from the area of fluorescence. (A-F) Nomarski optics, (a-f) same embryos, same stages as A-F, Epifluorescence. Factor of signal enhancement is given in top right corner. Bar: 10  $\mu$ m. Orientation: anterior, left.

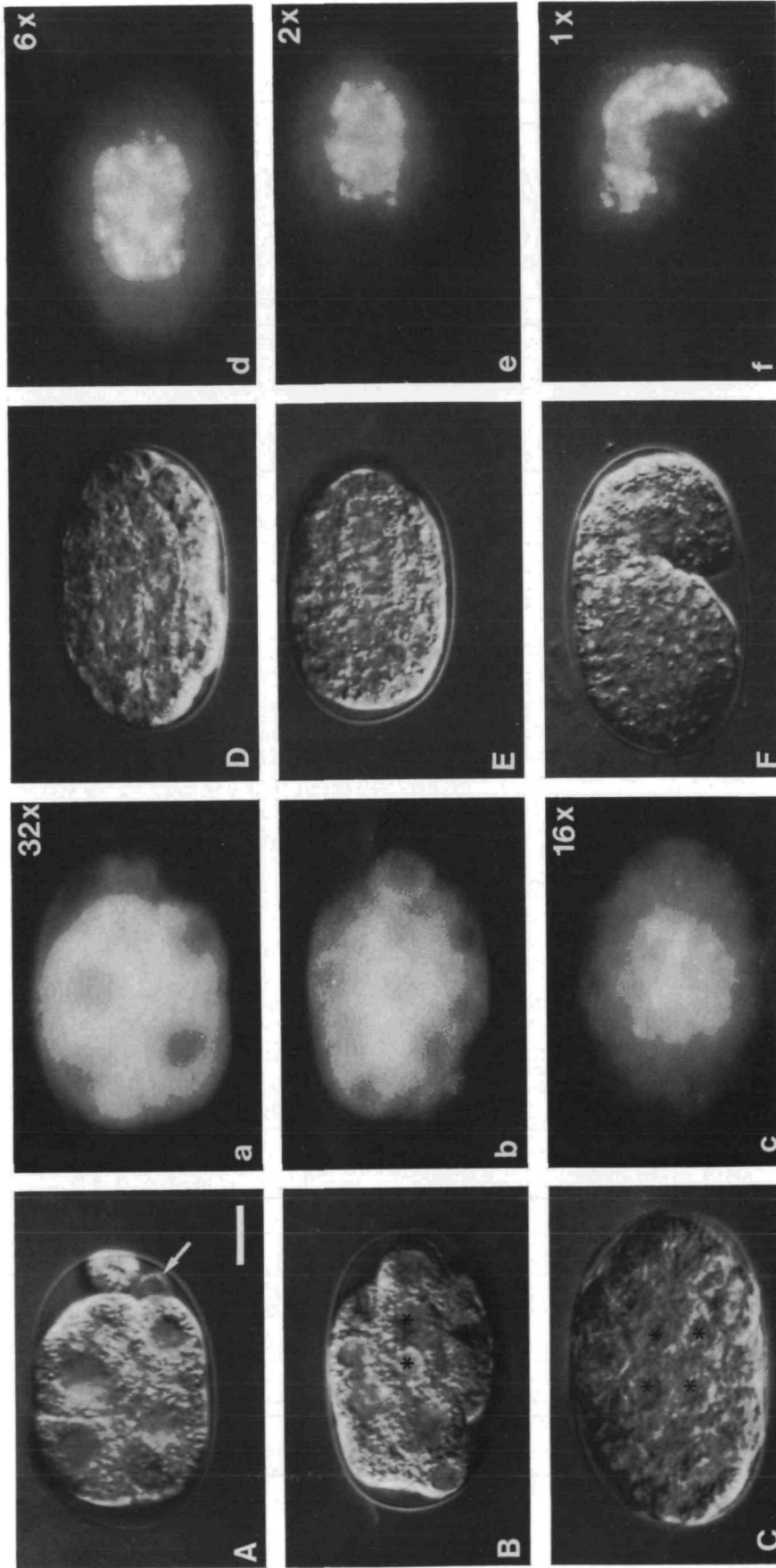


**Fig. 3.** Pattern of autofluorescence in the *Rh. dolichura* embryo. Similar stages as in Fig. 2. Differences in early cell pattern are due to species-specific variances in cell lineage. (A-F) 1 E-cell stage (A) to early morphogenesis phase (F), Nomarski optics. (a-f) Same embryo, same stages as A-F, epifluorescence.

Note fluorescence is absent in P<sub>4</sub> (a). Arrow marks the primordial germcell P<sub>4</sub>, asterisks mark the two (B) or four (C) E cells present at the respective stages. Factor of signal enhancement is given in top right corner. Bar: 10 μm; Orientation: anterior, left.

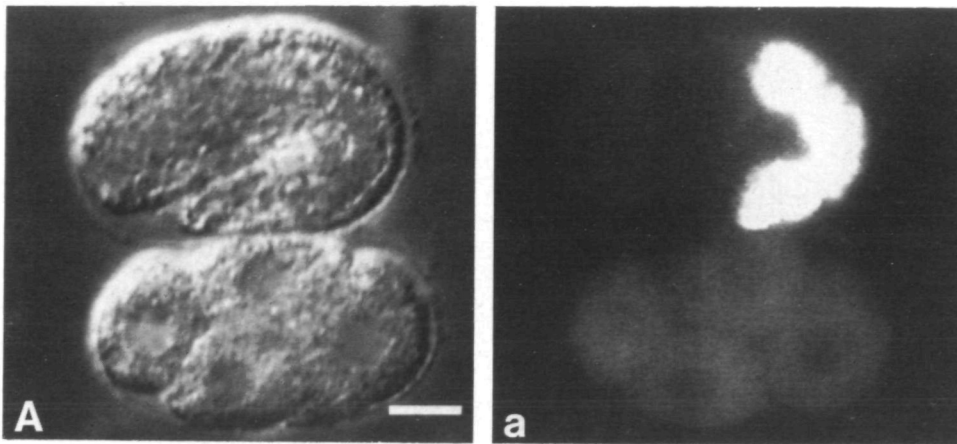


**Fig. 4.** Decreasing autofluorescence in non-gut cells of *Rh. dolichura*. (A) 4-cell stage (bottom) and morphogenesis stage (top); Nomarski optics. (a) Same embryos, same stages as in (A); autofluorescence. Note difference between early blastomeres and non-gut cells of morphogenesis stage. Enhancement 12 $\times$ . Bar: 10  $\mu$ m. Orientation: anterior, left (top embryo); anterior, right (bottom embryo).

can be detected also by direct observation (Fig. 3a). As reported above, fluorescence bleaches out very rapidly. In the 2 E-cell stage (<30 cells), fluorescent material starts to accumulate in the gut precursor cells (Fig. 3b), becoming granular in appearance and considerably stronger in the 4 E-cell stage (>40 cells, Fig. 3c). During embryogenesis the intensity of granular fluorescence in the gut primordium increases considerably (note declining factors of enhancement), while it disappears completely from all other cells (some pale background fluorescence remains; Fig. 3d-f). The intensity of autofluorescence in *Rh. dolichura* is several-fold higher than in *C. elegans* during all stages of embryogenesis.

To confirm that the apparent decrease in autofluorescence in the non-gut cells of *Rh. dolichura* is not simply the result of decreased signal enhancement, we recorded an early embryo together with a morphogenesis-stage embryo at the same enhancement factor (Fig. 4). While all cells of the early stage show some fluorescence, the non-gut cells of the late stage appear dark.

Two interpretations for the observations in *Rh. dolichura* appear possible. Either fluorescent material is produced in the intestine while at the same time it is degraded in all other tissues or else a transfer of fluorescent material into the gut primordium takes place. We therefore marked the egg cytoplasm of *C. elegans* with non-degradable fluorescent dyes.

#### *Lucifer Yellow indicates a transfer of cytoplasmic components into the gut primordium of C. elegans*

After microinjection of LYVS into selected blastomeres, the dye remains visible in the cytoplasm all through embryogenesis. If injected, for instance, into the AB cell of a 2-cell stage, LYVS (in contrast to another Lucifer dye, LYCH; our unpublished data) binds quickly to cytoplasmic particles and remains in the descendants of the injected cell (Fig. 5a, b). This finding could be explained by the rapid binding of LYVS or by the absence of functional communication channels at this stage. Towards the end of the proliferation phase, however, the dye was found to accumulate progressively in the differentiating gut

primordium, while disappearing correspondingly from the AB cells (Fig. 5c). Well before hatching, LYVS is essentially restricted to the gut (Fig. 5d). There the dye appears to accumulate in the autofluorescent granules because (viewed with the same excitation wavelength) they change in color from blue to yellowish. The same transfer phenomenon takes place if LYVS is injected into other non-gut precursor cells.

These data indicate that an intercellular transfer of molecules into the differentiating gut primordium takes place during embryogenesis in both *Rh. dolichura* and *C. elegans* in a similar fashion.

To characterize further the pathway of the tracer dye into the gut primordium, we tested whether the gut cells are able to take up the dye from the extracellular fluid of the perivitelline space.

#### *Laser-induced penetration of the eggshell demonstrates tissue- and stage-specific uptake of Lucifer Yellow*

The nematode embryo is surrounded by a prominent chitinous eggshell and an underlying thin vitelline membrane (lipid layer), the latter functioning as a chemical barrier (Bird, 1971). We penetrated the normally impermeable vitelline layer with a laser microbeam in a medium containing LYVS. If this is done in early stages, the dye fills the perivitelline space and surrounds the blastomeres but does not pass through the cell membranes (Stewart, 1978; Fig. 6a, b). However, during subsequent embryogenesis (from the 8 E-cell stage onwards; >200 cells) LYVS is specifically taken up by the cells of the gut primordium (Fig. 6c). This corresponds well to the developmental stage when normal autofluorescence becomes visible (Fig. 1) and may be explained by an endocytotic activity of the gut cells as part of their tissue-specific differentiation. Controls with intact morphogenesis-stage embryos preincubated with LYVS show the lining of the eggshell but no internal fluorescence (Fig. 6e). This demonstrates that it is not the arising gut-specific autofluorescence which is detected with the filter combination used to visualize LYVS.

To determine whether the observed uptake is a general, nonspecific process, we tested fluorescence dyes with chemical properties different from those of LYVS.

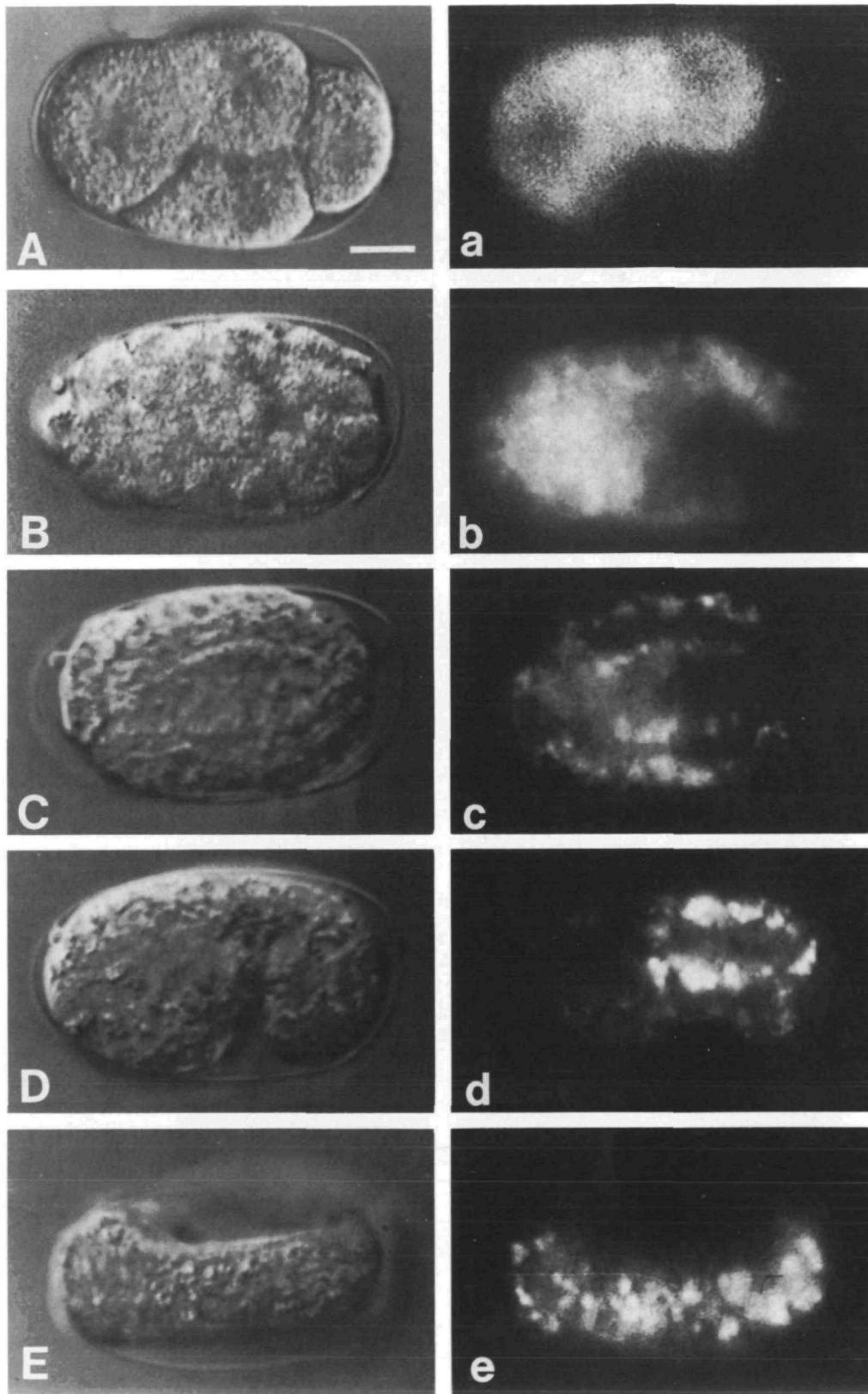


**Fig. 5.** Segregation of microinjected Lucifer Yellow in the *C. elegans* embryo. After injection of Lucifer Yellow into the AB cell of a 2-cell embryo, the dye distributes only to the descendants of the AB cell (A,a; B,b). During the morphogenesis stage the dye accumulates in the intestine and disappears from the AB descendants (D,d; E,e). (A-E) Nomarski optics; (a-e) same embryos, same stages, epifluorescence. Bar: 10  $\mu$ m. Orientation: anterior, left.

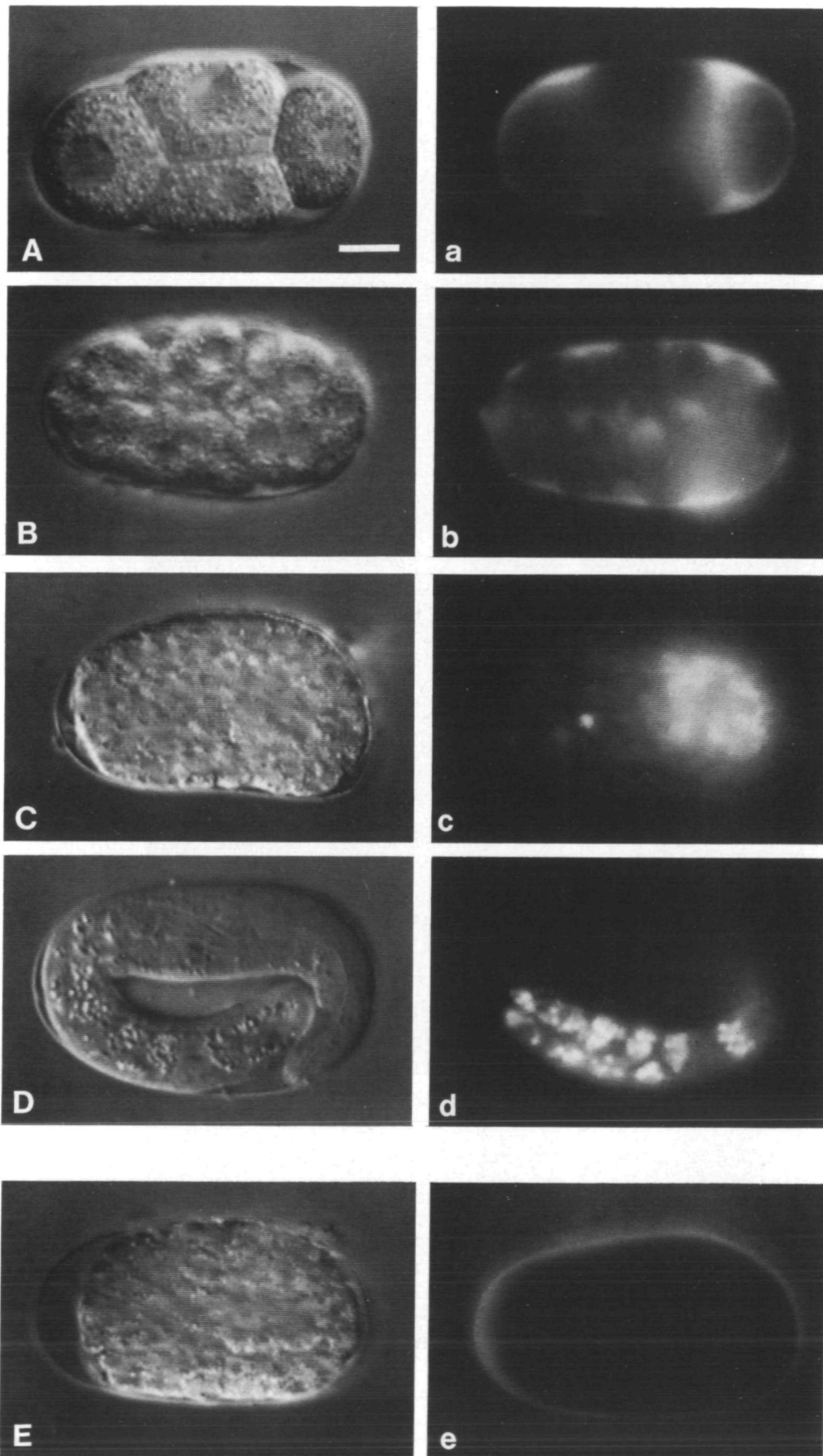


**Fig. 6.** Uptake of Lucifer Yellow from the perivitelline space in the *C. elegans* embryo. When the eggshell of an early embryo is penetrated with a laser microbeam in a medium containing LYVS, the dye fills the perivitelline space, but does not enter the cells (A,a, 4-cell stage; B,b, 26-cell stage). However, during later embryogenesis (C,c, Comma stage; D,d, Pretzel stage) LY accumulates exclusively in the intestine. Controls (eggshell not penetrated) analyzed with the same filter combination do not show gut-specific autofluorescence (E,e). A-E, Nomarski optics; a-e, Epifluorescence. Bar: 10  $\mu$ m. Orientation: anterior, left, except D,d.



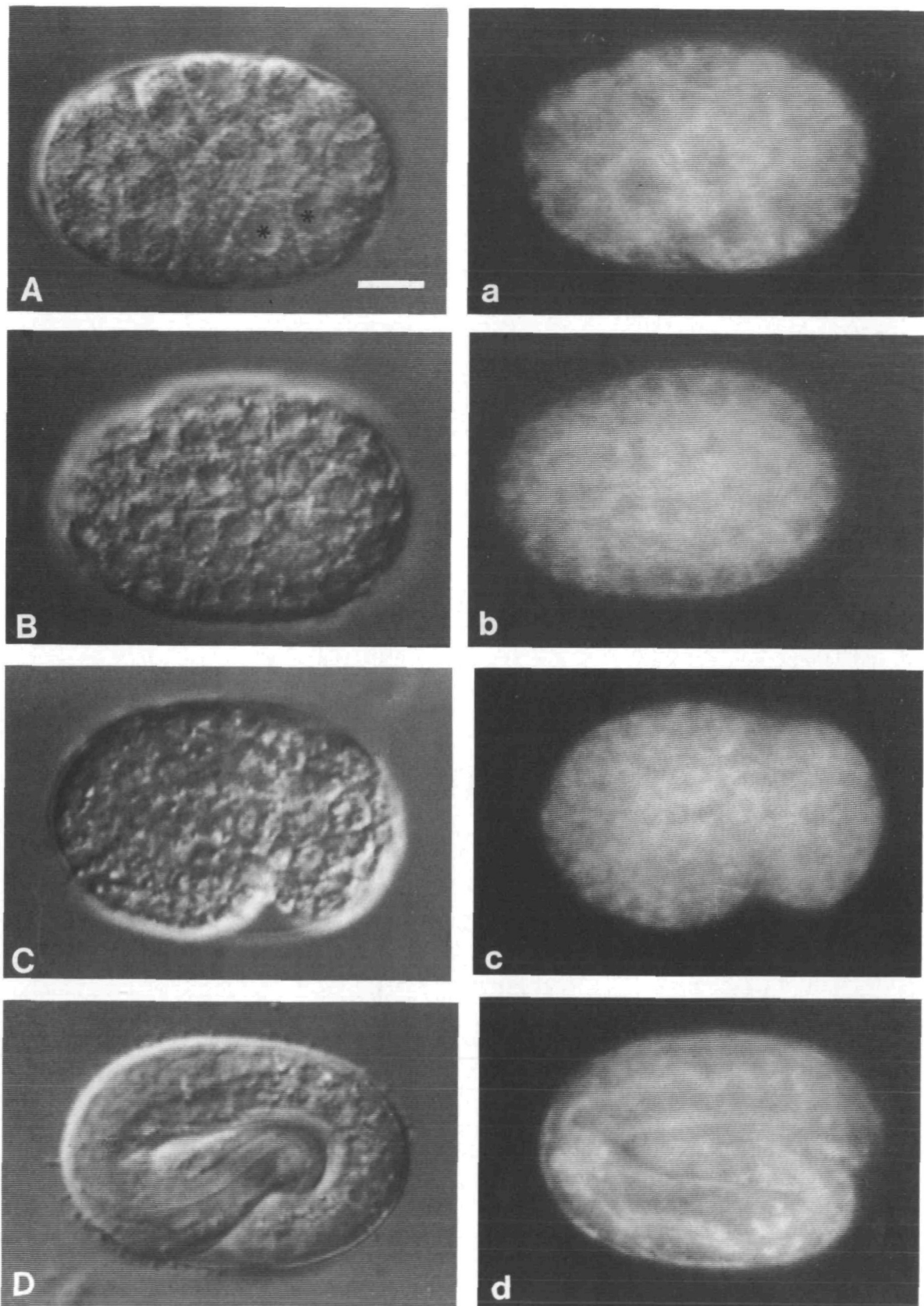


**Fig. 7.** Distribution of Rhodamine 6G during embryogenesis of *C. elegans*. (A,a) 2 E-cell stage, asterisks mark E cells. (B,b) 8 E-cell stage. (C,c) Early morphogenesis stage. (D,d) Late morphogenesis stage. (A-D) Nomarski optics, (a-d) same embryo, same stages as A-D, epifluorescence, enhancement 6 $\times$ . Bar: 10  $\mu$ m. Orientation: anterior, left.

*The pattern of Rhodamine-induced fluorescence does not change during embryogenesis of C. elegans*

After being labeled with  $10^{-4}\%$  R6G by feeding, embryos can develop normally, hatch and reproduce. At a tenfold higher concentration teratogenic effects are found. R6G is distributed into all tissues of the animals, including the gonad. In contrast to LYVS, the dye remains equally distributed over all cells during all phases of embryogenesis. No accumulation of R6G in the gut primordium takes place (Fig. 7A,a-D,d).

From these findings, we conclude that the intercellular transfer of marker dyes taking place in the nematode embryo has at least some specificity, apparently depending on the chemical properties of the dyes, possibly allowing differential binding to cytoplasmic components.

*Centrifugation demonstrates association of autofluorescence and vital dyes with distinct cytoplasmic fractions*

As described in more detail elsewhere (Schlicht and Schierenberg, 1991), centrifugation of nematode zygotes causes stratification of the cytoplasm into three distinct layers containing lipids (centripetal pole), clear cytoplasm (center), and yolk (centrifugal pole).

To test whether autofluorescent material and taken-up fluorescent dyes become associated with specific cytoplasmic layers, we centrifuged untreated *Rh. dolichura* and fluorescently labelled (LYVS; R6G; see Materials and methods) *C. elegans* embryos.

In the *Rh. dolichura* embryo, the bluish autofluorescence is mainly associated with yolk granules but is

also detectable in the fraction of the clear cytoplasm (Fig. 8a). In centrifuged *C. elegans* zygotes, a faint pale background fluorescence remains distributed over all cytoplasmic layers (data not shown) and therefore appears to be a general cytoplasmic property. LYVS-derived fluorescence is restricted to the region of the yolk granules at the centrifugal pole (Fig. 8b). R6G is especially associated with the fraction of the clear cytoplasm (Fig. 8c).

Our results suggest a specific binding of the applied fluorescence markers to different cytoplasmic components. The behavior of LYVS described above may well reflect a transfer of yolk components into the differentiating gut cells. If this turns out to be true, one would expect a significant increase in the volume of the developing gut primordium at the expense of the non-gut cells during the course of embryogenesis.

*Evidence for an increase in size of the gut primordium*

From 80-120 electron microscopical serial sections each through three early embryos of *C. elegans*, we calculated with the aid of a graphics tablet connected to a computer, the percentage of total egg volume occupied by the E cell (8-cell stage) or its two daughters (14- and 24-cell stages). For these three stages, we obtained very similar values of 10.8, 11.2 and 11.4%.

In the absence of section series through freshly hatched juveniles, we measured the relative areas of the intestinal cytoplasm (excluding the lumen) in 11 EM cross sections through various gut regions of a young L<sub>1</sub> stage larva. We obtained values between 40.5 and

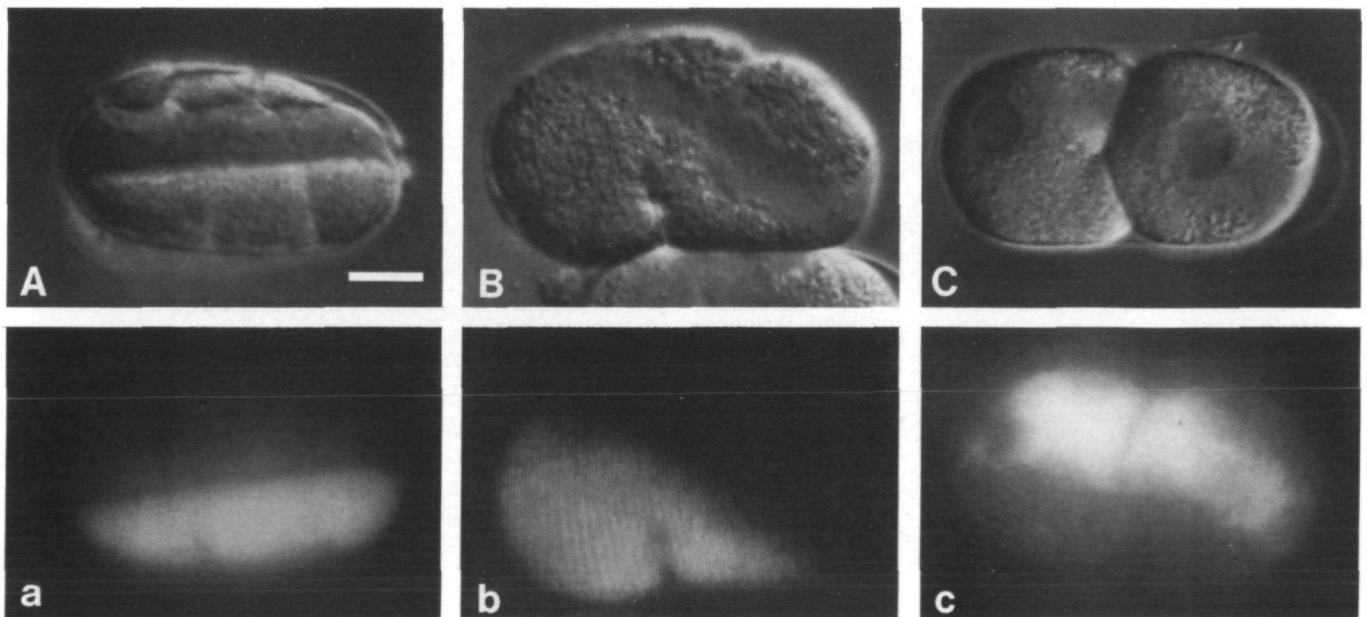


**Fig. 8.** Association of fluorescence markers with distinct cytoplasmic components after centrifugation of zygotes. (A,a) In *Rh. dolichura* bluish autofluorescence accumulates together with yolk granules at the centrifugal pole. (B,b) In *C. elegans* LYVS is exclusively associated with the fraction of yolk granules. (C,c) In *C. elegans* Rhodamine 6G is essentially found in the fraction of clear cytoplasm. (A-C) Normarski optics, (a-c) same embryos as A-C, epifluorescence. Bar: 10  $\mu\text{m}$ ; Orientation: centrifugal pole with yolk granules, bottom (a,c) or bottom left (b); centripetal pole with lipids, top (a,c) or top right (b).

49.1% (mean value: 44.6%). From five sections through different gut regions of a "pretzel stage", where the nearly complete worm is folded twice in the eggshell (as shown in Fig. 7D), we obtained values between 37.5% and 46.8% of total area (mean value: 40.8%). Our EM analysis has confirmed the previous view that the intestine can be viewed as a cylinder (see Sulston et al., 1983).

Measuring the length of the intestine of young first stage larvae ( $L_1$ ) with the light microscope, we obtained values between 50% and 54% (mean value: 52%;  $n=9$ ). Combining these data, we estimate the volume of the intestine in freshly hatched juveniles to be at least 20% of total animal volume. We assume this to be a rather conservative estimate because the portion taken up by the pseudocoelom was calculated as part of the non-gut cells.

In summary, we conclude from our measurements that the volume of intestinal cells in *C. elegans* roughly doubles during embryogenesis, while the embryo itself does not grow.

Expecting to make the inferred bulk accumulation of native material even more obvious, we blocked cleavage and looked to see whether the gut precursor cell increased in size during the period of normal embryogenesis.

It has been found in several different systems that tissue-specific differentiation of embryonic cells does not depend on cleavage (Whittaker, 1973; Laufer et al., 1980).

#### *Reversal of cell size relationship in cleavage-blocked 2-cell stages supports the assumption of a cytoplasmic transfer*

After permeabilizing the eggshell with a laser microbeam, we blocked cleavage in 2-cell embryos with Cytochalasin D. One of the two cells (the germline cell  $P_1$ ) is the precursor for the intestine (Boveri, 1899; Deppe et al., 1978), which can visibly differentiate by developing gut-specific autofluorescence without further division (Laufer et al., 1980).

In 20 out of 66 treated embryos, we found a clear reversal of cell size relationships that takes place during the subsequent 18-24 h. While the  $P_1$  cell (gut precursor) increases considerably in volume and expresses the typical autofluorescence, the originally larger AB cell decreases proportionally (Fig. 9). In a number of cases, we observed that the small AB cell had become practically devoid of granules while the  $P_1$  cell contained lots of these (data not shown). These findings give further evidence for the suspected massive intercellular transport of cytoplasmic components. In many embryos this process could not be demonstrated, largely because the detailed course of cell boundaries could not be identified clearly enough to judge whether an alteration in cell size had taken place. For the remainder, we assume that differentiation simply did not advance far enough, similar to what had been found by Laufer et al. (1980) in looking for the development of autofluorescence in cleavage-blocked 2-cell stages of *C. elegans*. The deduced transfer of cytoplasm appears

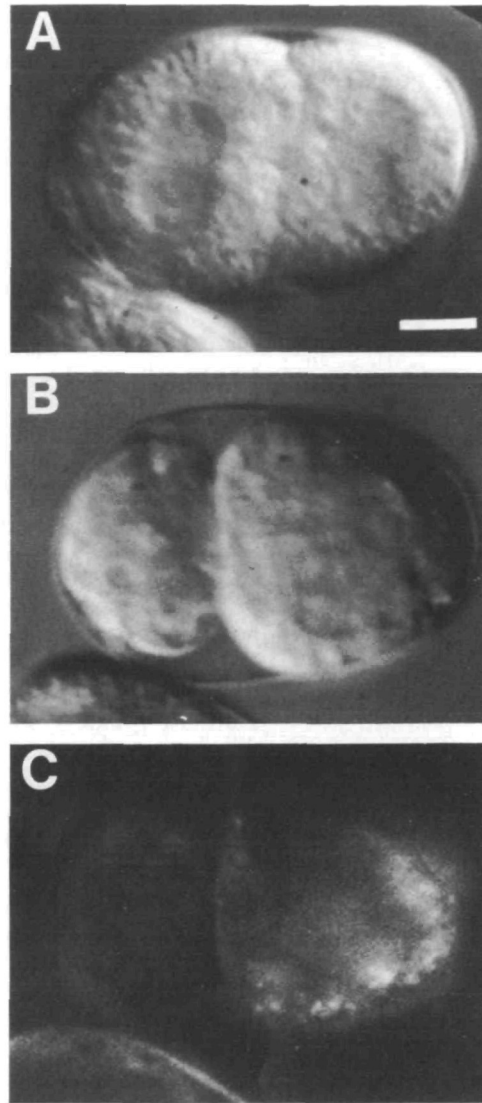


**Fig. 9.** Reversal of cell size relation in cleavage-blocked 2-cell embryos. (A) Divided nuclei in both cells about 15 minutes after start of cleavage block. The AB cell (left) is larger than  $P_1$  (right). (B) Terminal phenotype of the same embryo shown in A on next day. The  $P_1$  cell has become larger than AB. (C) Same embryo, same stage as in B, epi-illumination visualizing the pattern of autofluorescence. Bar: 10  $\mu\text{m}$ . Orientation: anterior, left.

not to take place via cytoplasmic bridges because fluoresceinated dextran ( $M_r$  4000) injected into one of the cells was found to remain restricted to it (data not shown).

#### **Discussion**

The results of this paper have been threefold. (1) We document the usefulness of a new commercially available low-cost image enhancement device for the detection of weak fluorescence. (2) We report novel observations concerning the origin and tissue-specific accumulation of autofluorescent material during em-

bryogenesis of the nematode *Rhabditis dolichura*. (3) We describe the suitability of certain vital dyes to visualize a prominent intercellular transfer process into the differentiating gut primordium of *Caenorhabditis elegans*.

We face two major difficulties in analyzing the fluorescence pattern in our test specimens. One of them is the low intensity and the rapid fading (photobleaching) in early embryos. The other is phototoxicity, the sensitivity of the nematode eggs to excitation with light of short wavelengths leading to developmental arrest probably potentiated by the dyes. Using a simple signal-enhancement device (in the price range of a conventional video camera), we can overcome these problems as documented above. For certain applications this can substitute for a severalfold more expensive light-intensifying camera. This unit has other applications where documentation of low-level fluorescence is critical, e.g. fluorescent antibodies.

The most straightforward interpretation of our results concerning the accumulation of autofluorescence or induced fluorescence in the two examined nematode species (Figs 3, 5, 6) is the assumption of a massive transfer of some cytoplasmic material from non-gut cells into the differentiating gut primordium. This view is supported by our calculation that the volume of the gut precursors in *C. elegans* approximately doubles during embryogenesis and the observation that a reversal of cell size relations takes place in cleavage-blocked 2-cell embryos (Fig. 9). The dramatic difference in the intensity of fluorescence between an early and a late stage embryo of *Rh. dolichura* (Fig. 4) indicates that regardless of the deduced transfer into the gut, large amounts of fluorescent material are being made over the course of embryogenesis.

Based on our findings that on the one hand the tracer dye LYVS is relocated from the AB cells into the gut primordium (Fig. 5) and on the other hand, is taken up by gut cells out of the perivitelline space (Fig. 6), we suggest that the inferred transfer of native material is accomplished in two steps: (1) exocytosis from non-gut cells into the perivitelline space and (2) endocytosis into the intestine. A comparable exo-/endocytosis process is initiated with the postembryonic transfer of yolk from its origin of production (intestine) via the body cavity into the oocytes (Kimble and Sharrock, 1983). Recently evidence has been presented that LY can utilize an organic anion transporter to cross cell membranes (Steinberg et al., 1987; O'Driscoll et al., 1991). For our case we consider this latter mechanism unlikely as we argue that LY is bound to cytoplasmic components.

Centrifugation experiments have revealed the association of LYVS and R6G with different cytoplasmic layers (Fig. 7). Despite a very similar  $M_r$  (457/479), the two dyes express a fundamentally different behavior with respect to accumulation in the gut cells. At the applied low centrifugal force (4500 g), one would in any case not expect the free dye molecules to be separated. Instead, LYVS and R6G appear to be bound to different cytoplasmic components, only one of which (that of LY) is transferred into the gut primordium.

The results of centrifugation indicate that both the bluish autofluorescence in *Rh. dolichura* and the tracer dye LYVS in *C. elegans*, are associated with yolk granules (Fig. 8). In insects, a degradation product of tryptophan catabolism, 3-hydroxykynurenine (which in *C. elegans* appears to be responsible for the bluish autofluorescence; Siddiqui and Babu, 1980), is coupled to yolk. In *Rh. dolichura* this degradation product may either be synthesized already in the oocyte and coupled to yolk or may be transferred together with yolk components out of the intestine into the gonad. In the egg of *C. elegans*, this autofluorescent component is either present only in extremely low amounts or restricted to the intestine. While in insects kynurenine is used for eye pigmentation and represents excretion and storage products (Linzen, 1974), we are not aware of any reports of a specific role for this molecule in nematode development.

The variance between the two analyzed nematode species with respect to when and where autofluorescence becomes visible and its intensity may be due to only minor genetic differences. In *C. elegans*, mutations in a single gene (leading to a preference for one of the alternative degradation pathways of tryptophan; Babu, 1974) result in a stronger intensity of fluorescence, which therefore becomes visible earlier than normal (Siddiqui and von Ehrenstein, 1980). Very recently embryonic arrest mutants in *C. elegans* have been isolated, which do not develop autofluorescent gut granules (J. Shaw, personal communication). Such mutants may help to understand better the transfer processes described here.

Another clue that autofluorescence is associated with yolk is given by our observation that in *Rh. dolichura*, the primordial germcell P<sub>4</sub> receives only very little granular material and does not express any detectable bluish autofluorescence even after enhancement (Fig. 3).

Further support for our idea that LYVS is bound to yolk components and marks their way into the gut is given by our finding that the patterns of LY-induced fluorescence in embryos (Fig. 2) and maturing oocytes (data not shown) of *C. elegans* look very much like those after staining with an antibody against a major yolk protein (Sharrock, 1983; our unpublished data). From other systems it has also been reported that LY binds to yolk proteins (Danilchik and Gerhart, 1987; Opresko and Karpf, 1987).

Seeking an explanation for the high concentration of yolk in the gut of the late embryo of *C. elegans*, Sharrock (1983) speculated that the intestine may store yolk as an energy source for postembryonic development. Our preliminary data support this view. We have found that freshly hatched juveniles can survive in buffer for at least a week without food, losing most of their yolk reserve during this time (data not shown). The observed fluorescence patterns may thus visualize an export of yolk not needed during embryogenesis. In a variety of different systems, it has been shown that only limited degradation of yolk proteins during embryogenesis takes place and the bulk part is still

present in the larva (Karasaki, 1963; Chinzei and Yano, 1985; Armant et al., 1986; Yamashita and Indrasith, 1988; Scott et al., 1990).

As we have shown, the final destination of LYVS is in the autofluorescent gut granules of the late embryo (Fig. 6). In the adult hermaphrodite of *C. elegans*, the blue autofluorescent pigments in the intestinal cells share properties with secondary lysosomes (Clokey and Jacobson, 1986). This is also true for the late embryo, where the lipophilic weak base Neutral Red marks the same granules (our unpublished results). Thus, the yolk components marked by LYVS appear to be taken up into intestinal lysosomes, where further degradation may take place.

During the second half of embryogenesis, certain hypodermal cells show an apparent accumulation of granules (Sulston et al., 1983), which seem to contain yolk as visualized by an anti-vitellogenin antibody (data not shown). However, as we could not detect any uptake of LYVS from the perivitelline space into these cells, we assume that they just retain their original material. This becomes more prominent with the typical flattening of the hypodermal cells (Priess and Hirsh, 1986). The reported diminution of refractile granules in the intestine (Sulston et al., 1983) may be explained by the fusion of lysosomes to yolk granules (Perona et al., 1988). This idea is supported by the appearance and continuous increase of large autofluorescent and birefringent gut granules during later morphogenesis (Chitwood and Chitwood, 1950; Laufer et al., 1980).

In uncleaved eggs of various species, yolk is found to be concentrated in the vegetal region of the uncleaved egg (Balinsky, 1975). In other systems such as the annelid *Nereis*, it has been shown that during early cleavage essentially all yolk is segregated into the large vegetal macromeres which generate the gut (Wilson, 1892; Dorresteyn, 1990). The fact that different mechanisms (prelocalization; segregation; transfer) lead to a similar result (accumulation of yolk in the gut primordium) may reflect a more general developmental principle.

Finally, we wonder whether the observed uptake of molecules from the extracellular space into the intestine (Fig. 6) is restricted to embryogenesis or continues postembryonically. Preliminary experiments with injected marker dyes indicate that intestinal cells of adults not only take up substances from the gut lumen but also from the surrounding body cavity.

We thank Thomas S. Cole for electron microscopy, Frauke Skiba for the *Rh. dolichura* strain, and Randall Cassada for critical reading of the manuscript. This work was supported by a grant of the Deutsche Forschungsgemeinschaft to E.S. (Schi 214/2-2).

## References

- Armant, R. D., Carson, D. D., Decker, G. L., Welply, J. K. and Lennarz, W. J. (1986). Characterization of yolk platelets isolated from developing embryos of *Arbacia punctulata*. *Devl Biol.* 113, 342-355.
- Babu, P. (1974). Biochemical genetics of *Caenorhabditis elegans*. *Molec. Gen. Genet.* 135, 39-44.
- Balinsky, B. I. (1975). *An Introduction to Embryology*, 4th edition. Philadelphia: W.B. Saunders.
- Bird, A. F. (1971). *The Structure of Nematodes*. New York: Academic Press.
- Boveri, T. (1899). Die Entwicklung von *Ascaris megaloccephala* mit besonderer Rücksicht auf die Kernverhältnisse. In *Festschrift Kupffer*, pp. 383-430, Jena: Fischer.
- Brenner, S. (1974). The genetics of *Caenorhabditis elegans*. *Genetics* 77, 71-94.
- Chinzei, Y. and Yano, I. (1985). Vitellin is the nutrient reserve during starvation in the nymphal stage of a tick. *Experientia* 41, 948-950.
- Chitwood, B. G. and Chitwood, M. B. (1950). *Introduction to Nematology* (Reprinted 1974) Baltimore: University Park Press.
- Clokey, G. V. and Jacobson, L. A. (1986). The autofluorescent "lipofuscin granules" in the intestinal cells of *Caenorhabditis elegans* are secondary lysosomes. *Mech. Ageing Dev.* 35, 79-94.
- Cole, T. S. and Schierenberg, E. (1986). Laser microbeam-induced fixation for electronmicroscopy: Visualization of transient developmental features in nematode embryos. *Experientia* 42, 1046-1048.
- Danilchik, V. M. and Gerhart, J. C. (1987). Differentiation of the animal-vegetal axis in *Xenopus laevis* oocytes. I. Polarized intracellular translocation of platelets establishes the yolk gradient. *Devl Biol.* 122, 101-112.
- Deppe, U., Schierenberg, E., Cole, T., Krieg, C., Schmitt, D., Yoder, B. and von Ehrenstein, G. (1978). Cell lineages of the embryo of the nematode *Caenorhabditis elegans*. *Proc. natn. Acad. Sci. USA* 75, 376-380.
- Dorresteyn, A. W. C. (1990). Quantitative analysis of cellular differentiation during early embryogenesis of *Platynereis dumerilii*. *Roux's Arch. Devl Biol.* 199, 14-30.
- Edgar, L. G. and McGhee, J. D. (1986). Embryonic expression of a gut-specific esterase in *Caenorhabditis elegans*. *Devl Biol.* 114, 109-118.
- Edgar, L. G. and McGhee, J. D. (1988). DNA synthesis and the control of embryonic gene expression in *C. elegans*. *Cell* 53, 589-599.
- Karasaki, S. (1963). Studies on amphibian yolk. Electron microscopic observations on the utilization of yolk platelets during embryogenesis. *J. Ultrastruct. Res.* 9, 225-247.
- Kimble, J. and Sharrock, W. J. (1983). Tissue-specific synthesis of yolk proteins in *Caenorhabditis elegans*. *Devl Biol.* 96, 189-196.
- Laufer, J. S., Bazzicalupo, P. and Wood, W. B. (1980). Segregation of developmental potential in early embryos of *Caenorhabditis elegans*. *Cell* 19, 569-577.
- Laufer, J. S. and von Ehrenstein, G. (1981). Nematode development after removal of egg cytoplasm: Absence of localized unbound determinants. *Science* 211, 402-404.
- Linzen, B. (1974). The tryptophan => ommochrome pathway in insects. *Adv. Insect Physiol.* 10, 117-246.
- O'Driscoll, D., Wilson, G. and Steer, M. W. (1991). Lucifer Yellow and fluorescein isothiocyanate uptake by cells of *Morinda citrifolia* in suspension cultures is not confined to the endocytotic pathway. *J. Cell Sci.* 100, 237-241.
- Opreško, L. K. and Karpf, R. A. (1987). Specific proteolysis regulates fusion between endocytic compartments in *Xenopus* oocytes. *Cell* 51, 557-568.
- Perona, R., Bes, J.-C. and Vallejo, C. G. (1988). Degradation of yolk in the brine shrimp *Artemia*. Biochemical and morphological studies on the involvement of the lysosomal system. *Biol. Cell* 63, 361-366.
- Priess, J. R. and Hirsh, D. I. (1986). *Caenorhabditis elegans* morphogenesis: the role of the cytoskeleton in elongation of the embryo. *Devl Biol.* 117, 156-173.
- Schierenberg, E. (1978). Die Embryonalentwicklung des Nematoden *Caenorhabditis elegans*. Ph.D. thesis. University of Göttingen.
- Schierenberg, E. and Wood, W. B. (1985). Control of cell-cycle timing in early embryos of *C. elegans*. *Devl Biol.* 107, 337-354.
- Schlicht, P. and Schierenberg, E. (1991). Establishment of cell lineages in the *C. elegans* embryo after suppression of the first cleavage: Support for a concentration-dependent decision mechanism. *Roux's Arch. Devl Biol.* 199, 437-448.

- Scott, L. B., Lennarz, W. J., Raff, R. A. and Wray, G. A. (1990). The "lecithotrophic" sea urchin *Heliocidaris erythrogramma* lacks typical yolk platelets and yolk glycoproteins. *Devl Biol.* **138**, 188-193.
- Sharrock, W. J. (1983). Yolk proteins of *Caenorhabditis elegans*. *Devl Biol.* **96**, 182-188.
- Siddiqui, S. S. and Babu, P. (1980). Genetic mosaics of *Caenorhabditis elegans*: A tissue-specific fluorescent mutant. *Science* **210**, 330-332.
- Siddiqui, S. S. and von Ehrenstein, G. (1980). Biochemical genetics of *C. elegans*. In *Nematodes as Biological Models*, vol. 1 (ed. B. Zuckerman), pp. 285-312. New York: Academic Press.
- Steinberg, T. H., Newman, A. S., Swanson, J. A. and Silverstein, S. C. (1987). Macrophages possess probenecid-inhibitable organic anion transporters that remove fluorescent dyes from the cytoplasmic matrix. *J. Cell Biol.* **105**, 2695-2702.
- Stewart, W. W. (1978). Functional connection between cells as revealed by dye-coupling with highly fluorescent naphthalimide tracer. *Cell* **14**, 741-759.
- Sulston, J. E. and Horvitz, H. R. (1977). Post-embryonic cell lineages of the nematode *Caenorhabditis elegans*. *Devl Biol.* **56**, 110-156.
- Sulston, J. E., Schierenberg, E., White, J. and Thomson, N. (1983). The embryonic cell lineages of the nematode *Caenorhabditis elegans*. *Devl Biol.* **100**, 64-119.
- Whittaker, J. R. (1973). Segregation during ascidian embryogenesis of egg cytoplasmic information for tissue-specific enzyme development. *Proc. natn. Acad. Sci. USA* **70**, 2096-2100.
- Wilson, E. B. (1892). The cell-lineage of *Nereis*. A contribution to the cytogeny of the annelid body. *J. Morph.* **6**, 361-480.
- Yamashita, O. and Indrasith, L. S. (1988). Metabolic fates of yolk proteins during embryogenesis in arthropods. *Develop. Growth and Differ.* **30**, 337-346.

(Accepted 29 October 1991)